

Received 27 August 2023, accepted 21 October 2023, date of publication 30 October 2023, date of current version 3 November 2023.

Digital Object Identifier 10.1109/ACCESS.2023.3328335

## RESEARCH ARTICLE

# Study on the Maximum Ice-Shedding Height of Conductor Based on Energy Method

JINYU WANG<sup>1</sup>, ZHITAO YAN<sup>2</sup>, YONGLI ZHONG<sup>1,2</sup>, MING LU<sup>1</sup>, ZHE LI<sup>1</sup>, AND BIN LIU<sup>3</sup>

<sup>1</sup>Electric Power Research Institute, State Grid Henan Electric Power Company, Zhengzhou 450052, China

<sup>2</sup>School of Civil Engineering and Architecture, Chongqing University of Science and Technology, Chongqing 401331, China

<sup>3</sup>China Electric Power Research Institute, Beijing 100055, China

Corresponding author: Yongli Zhong (zhongyongli@cqust.edu.cn)


This work was supported in part by the National Natural Science Foundation of China under Grant 52178458 and Grant 52008070, in part by the Project of State Grid Henan Electric Power Company under Grant 52170223000Q, in part by the Natural Science Foundation of Chongqing Municipality under Grant CSTB2022NSCQ-MSX0363, and in part by the Project funded by the China Postdoctoral Science Foundation under Grant 2023M734084.

**ABSTRACT** Ice shedding of transmission lines may lead to interphase flashover and thereby endanger power transmission. The ice shedding of transmission lines is essentially an energy conversion process. Based on the vibration theory and energy method of cable structures, the iced load of a transmission line is regarded as the working load under the condition of a bare conductor. The theoretical analysis model of ice shedding for a single-span transmission line was established with a vertical symmetrical vibration mode configuration. Then the analytical solution of maximum jump height is given. The proposed formula makes clear the quantitative relationship among maximum jump height and the verticality of the conductor, the icing mass ratios, and the dimensionless frequency. The vibration of a single-span transmission line after ice shedding is investigated by the finite element method to validate the proposed formula. The results show that the maximum jump height calculated by the formula has a good agreement with the finite element analysis, which fully meets the engineering accuracy requirements. The total jump height calculated by the current method is only 1.6% lower than that from finite element method. The contribution of high-order vertical mode is small with a small sag. By considering the contribution of high-order vertical modes, the calculation formula was further modified to get more accurate results. Since the vertical modes are mainly determined by dimensionless parameters, a simplified calculation empirical formula for maximum jump height optimization was obtained by fitting based on parametric analysis results. The presented proposed formula can provide theoretical guidance and be employed to predict the maximum jump height after ice shedding for transmission line design.

**INDEX TERMS** Transmission line, ice shedding, energy method, maximum jump height, analytical formula.

## I. INTRODUCTION

The high-voltage transmission tower-line system plays a crucial role in social and economic development. Electricity is carried from the source of power generation to the distribution system by Transmission Lines (TLs). Most failures of TLs in China are due to extreme events, including icing caused by low temperature, High-Intensity Wind (HIW) events (downbursts and Tornadoes) [1], [2], [3], [4]. The interruption of electricity due to the failure of TLs is unacceptable from the

The associate editor coordinating the review of this manuscript and approving it for publication was Ali Raza .

standpoint of both social and economic losses. TLs with large pitch and high flexibility show obvious nonlinear vibration characteristics during the vibration process of icing and de-icing. Ice shedding can cause significant vertical vibration of the conductor and unbalanced tension on the support tower [5]. Excessive vertical vibration displacement may cause interphase flashover accidents, and unbalanced tension can cause the collapse of transmission towers. Therefore, it is necessary to investigate the largest jump height of the conductor and the unbalanced tension.

The nonlinear characteristics of conductors lead to coupling effects during vibration, which brings great difficulties

to the research on the vibration of conductors after ice shedding. In recent years, experimental tests and numerical simulation are the main methods to investigate the jump height of TLs after ice shedding. Morgan and Swift [6] conduct early experimental research on the vibration of a multi-span transmission line after the sudden release of ice loads. Based on the experimental results, they indicated that only by ensuring sufficient horizontal spacing between the two phases can flashover be prevented. After that, researchers modeled ice shedding experimentally with comprehensive parameters, such as ice thickness, line characteristics, span length, the elevation difference between the dead-end and suspension point [7], ice-shedding scenarios [8], elevation difference, initial stress in sub conductors, accreted ice thickness [9] and the number of spans. In addition, most experimental studies did not consider the effects of wind loads. Liu et al. [10] conducted a three-span reduced-scale model test in wind tunnel to investigate the jump height, tension force of the conductors, and axial force changes of insulators after ice-shedding. They found that ice-shedding vibration is affected by the aerodynamic damping of conductors. The maximum jump height and vibration period become smaller with wind loads. The conductor tension force and insulator axial force increase with the increase in wind velocity. The above research on the vibration of TLs after ice shedding is mostly based on the modeling analysis of a certain independent pitch line, focusing on the discussion of the dynamic response after deicing, and further research is needed to realize the fast and accurate calculation of deicing jump height.

The cost of conducting deicing experiments on actual TLs is usually too expensive [11]. Due to the nonlinearity of TLs and other limitations, there are significant differences between the results obtained from scaled tests and the actual situation [9], [12]. With the development of computer technology, numerical simulation based on the finite element method (FEM) was gradually employed in the dynamic analysis of TLs after ice-shedding. Jamaledine et al. [13] used ADINA to investigate the non-linear dynamic response of TLs and compared the numerical results to their experiment. They indicated that ADINA has excellent performance in simulating this highly nonlinear vibration of TLs after ice-shedding. After that, ADINA was used by Kollar and Farzaneh [14] to simulate the vibration response of TLs after ice shedding with additional force. The simulation results show that the shock absorber can reduce the vibration jump height of the de-icing vibration. In the past decade, researchers have more widely used finite element methods to study the jump height and tension of TLs with various ice-shedding and structural parameters [8], [15], [16], [17], [18], [19], [20], [21]. In addition, machine learning is a new method to study the dynamic response of TLs after ice-shedding [8], [12], [22]. Researchers first conducted extensive FEM calculations to create a dataset including the maximum jump height, horizontal swing, and unbalanced tension of transmission lines under different structural, ice,

and wind parameters. The prediction models can be constructed based on the dataset and can be helpful in the design of TLs in ice zones.

Numeric calculation methods have yielded many useful results and conclusions, but in engineering applications, formulas are still needed for the design of TLs. Compared to experimental and numerical research, the theoretical work on the jumping height of TLs after ice-shedding has received less attention. Oertli [23] proposed an integral formula to calculate the jump height of the wire after deicing without considering the suspension point displacement of the insulator string and the change of wire tension. List and Pochop [24] proposed an approximate calculation formula for deicing jump related to density per unit length of wire, elastic modulus, and tensile stress. In the Chinese design code for overhead TLs [25], the suggested formula for the estimation of maximum jump height depends on the sag difference before and after ice-shedding. It is worth noting that the calculation formula of maximum jump height is based on simplified theory, experience, or a specific test, without considering the effect of different structural parameters and deicing loads in actual TLs. Therefore, Yan et al. [15] proposed a simplified formula to calculate the maximum jump height based on numerical simulation results with ABAQUS and data fitting. Wu et al. [18] established a theoretical model of deicing jump height of ice-covered transmission lines, but only considered the energy relationship under static state, and its extensive engineering applicability remains to be determined. Xie et al. [26] established a quantitative relationship between jump height and sag based on the parabola, but the formula contained tension in different states and did not consider the influence of cable dynamic characteristics. Lou et al. [27] obtain aerodynamic force coefficients of the iced conductor with crescent sections by wind tunnel experiment. Based on the FEM results, they proposed an empirical formula for estimating the maximum height jump considering the combined effect of ice and wind. In most of the above theoretical studies on the vibration of TLs after ice shedding, a simplified approximate formula was proposed based on fitting the results of experiments or numerical simulation, or only the results of static state were considered. Current existing theoretical models also lacked clear mathematical and physical significance.

In this paper, based on the basic theory of cable structures, the energy method is used to establish a simplified model to estimate the maximum jump height for single-span TLs, and the loads from ice shedding of TLs are regarded as the external load in the uniced state. The proposed analytical calculation formula can give a reference for the design of TLs. It is worth noting that the theoretical derivation of deicing vibration in this paper is carried out by taking a single conductor as an example. For multi-span and multi-bundles conductors, it is only necessary to change the boundary conditions of cable to lead model variations, Then the model proposed in this paper is also applicable.

## II. ANALYSIS OF THE MECHANICAL STATE OF ICE-COVERED TLS DEICING

In order to study the dynamic response of TLs after ice-shedding, it is assumed that the deicing process was divided into four states, as shown in Figure 1. In the state I, the transmission line is not covered with ice. TLs take on a catenary shape with the action of gravity. Considering the boundary conditions of TLs, the catenary equation of the TLs at the same height can be obtained [28]:

$$z = \frac{\sigma_0}{mg} \left( \operatorname{ch} \frac{mg}{\sigma_0} (x - l/2) - 1 \right) \quad (1)$$

where  $m$  is the mass per unit length of the transmission line,  $g$  is the acceleration of gravity and  $\sigma_0$  is the initial stress. In status II, the TLs are in static equilibrium after icing. Under the action of gravity from TLs and covered ice, the TLs sag with a displacement  $\Delta d$ . In State III, the TLs jump after ice-shedding, and at a certain time step, the TLs reach the maximum jump height. In state IV, the transmission line reaches a stable equilibrium position after a long time of vibration attenuation. If the covered ice on TLs is completely detached, state IV eventually coincides with state I.

Generally, the vibration after ice-shedding focuses on the displacement difference from state II to state III in previous research and engineering applications [22], [29], [30]. Considering that the displacement at the midpoint of the span is usually the largest, the displacement at the midpoint of the span is taken as the maximum jump height  $A$ , which can be composed of the displacement  $\Delta d$  from state I to state II and the displacement  $A_0$  from state I to state III. According to the energy conservation law for an elastic conductor system, the work done by icing on the transmission line is equal to the sum of the system strain energy and the increment of gravitational potential energy after ice-shedding. The maximum jump height  $A_0$  of the TLs can be derived. In order to simplify the derivation, it can be assumed that the TLs are arranged horizontally, and the deicing scenario is the whole span ice-shedding. For non-horizontal transmission lines, a similar derivation can be achieved by rotating the coordinate system. For partial ice-shedding, energy integration for partial sections of the TLs span can also be used.

## III. THE RELATIONSHIP MODEL BETWEEN DYNAMIC TENSION AND MAXIMUM JUMP HEIGHT

### A. VIBRATION EQUATION OF ICE-COVERED TLS AFTER ICE-SHEDDING

Considering the state I of TLs: the motion state of the horizontally ice-covered TLs hinged at both ends is shown in Figure 1, and the motion equation is:

$$\frac{\partial}{\partial s} \left\{ (T + \tau) \left( \frac{dz}{ds} + \frac{\partial w(x, t)}{\partial s} \right) \right\} = m \frac{\partial^2 w(x, t)}{\partial t^2} - mg \quad (2)$$

where  $w(x, t)$  is the vertical displacement of the transmission line,  $T$  is the tension in the transmission line,  $\tau$  is the dynamic tension of the transmission line,  $m$  is the mass per unit length of the transmission line before icing (or after

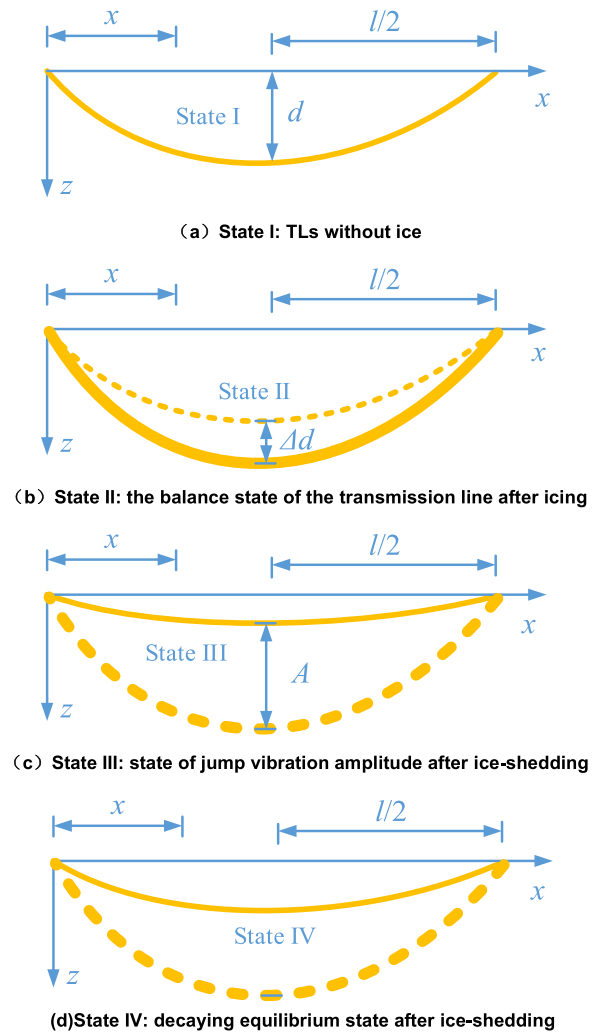


FIGURE 1. Four states of TLs before and after ice-shedding.

ice-shedding), and  $g$  is the acceleration of gravity. If the ice-covered transmission line is considered to be a small sag cable (the vertical-span ratio is less than 8), according to Newton's second law, the dynamic equations in vertical and horizontal directions can be written, respectively, as

$$T \frac{dx}{ds} = H \quad (3)$$

$$\frac{d}{ds} \left\{ T \frac{dz}{ds} \right\} = -mg \quad (4)$$

Substitute Eqs. (3) and (4) into Eq. (2), one obtains:

$$H \frac{\partial^2 w(x, t)}{\partial s^2} + h \frac{d^2 z}{dx^2} = m \frac{\partial^2 w(x, t)}{\partial t^2} \quad (5)$$

where  $H$  is the horizontal tension of the uniced transmission line, and  $h$  is the horizontal tension relative to the transmission line before icing.

### B. TENSION AND DISPLACEMENT IN ICE-COVERED TLS (STATE II)

The initial tension and initial configuration can be determined according to Eq. (1). After the transmission line is covered

with ice, the tension and displacement of the line change from state I to state II, and the displacement can be calculated according to Eq. (6) [20].

$$w = \frac{1}{2(1+h)} \left(1 - \frac{h}{p}\right) x(1-x) \quad (6)$$

where  $w = w/(m_1gl/H)$  is the dimensionless parameter of the displacement of the transmission line,  $h = h/H$  is the ratio of the transmission line tension  $h$  to the horizontal initial tension  $H$ ,  $x = x/l$  is the dimensionless horizontal coordinates,  $p = m_1/m$  represents the ratio of the ice-covered mass  $m_1$  per unit length to the mass  $m$  of the conductor before ice-covered. The horizontal tension can be obtained according to the balance equation (7) of the cable [28]:

$$\frac{hL_e}{EA} = - \int_0^l \left( \frac{d^2z}{dx^2} + \frac{1}{2} \frac{d^2w}{dx^2} \right) w dx \quad (7)$$

Substituting Eqs. (1) and (6) into Eq. (7), the analytical expression of tension can be obtained as follow:

$$h^3 + \left(2 + \frac{\lambda^2}{24}\right) h^2 + \left(1 + \frac{\lambda^2}{12}\right) h - \frac{\lambda^2}{12} p \left(1 + \frac{p}{2}\right) h = 0 \quad (8)$$

where,  $\lambda^2 = \frac{(mg)^2 l^3 EA_r}{H^3 l_e}$  is a dimensionless parameter, if small deformation is considered, then  $\lambda^2 = \frac{64EA_r}{H} \left(\frac{d}{l}\right)^2$ .  $E$  is the elastic modulus of the conductor,  $A_r$  is the cross-sectional area,  $l$  is the horizontal span length of TLLs,  $d$  is the initial sag of TLLs, and  $l_e$  is the arc length of TLLs.

### C. MAXIMUM JUMPING HEIGHT AFTER ICE-SHEDDING

In state III, the motion of the transmission line after ice-shedding is generally vertical vibration. Assuming that the conductor vibrates according to the first-order vertical symmetry mode after ice-shedding, the dynamic tension is approximately constant along the span length direction ( $x$ -direction).

Assuming that  $w(x, t) = \tilde{w}(x) e^{i\omega t}$ ,  $h(t) = \tilde{h} e^{i\omega t}$ , substituting them into Eq. (5), one can obtain:

$$H \frac{\partial^2 \tilde{w}}{\partial s^2} + m\omega^2 \tilde{w} = \frac{mg}{H} \tilde{h} \quad (9)$$

It is obvious that the dimensionless solution of Eq. (9) is:

$$\tilde{w} = \frac{\tilde{h}}{\omega^2} \left(1 - \tan \frac{\omega}{2} \sin \omega x - \cos \omega x\right) \quad (10)$$

Dimensionless parameters are used here. In Eq. (10),  $\tilde{w} = w/(mgl^2/H)$  represents the movement displacement of the transmission line after ice shedding,  $\tilde{h} = h/H$  and  $\omega = \omega l/(H/m)^{1/2}$  are dimensionless dynamic tension and vibration frequency, respectively.  $\omega$  is the vertical vibration circular frequency of the transmission line, which can be solved by the following transcendental equation.

$$\tan \frac{\omega}{2} = \frac{\omega}{2} - \frac{4}{\lambda^2} \left(\frac{\omega}{2}\right)^3 \quad (11)$$

### D. DYNAMIC TENSION AFTER ICE SHEDDING

The transmission conductor vibrates freely after ice shedding. It can be assumed that the maximum jump height of the midpoint ( $x = 0.5l$ ) between state I and state III of the uniced conductor is  $A_0$ , which can be obtained by substituting  $x = 0.5l$  into Eq. (10).

$$h = \omega^2 / \left(1 - \tan \frac{\omega}{2} \sin \frac{\omega}{2} - \cos \frac{\omega}{2}\right) / (mgl^2/H) A_0 \quad (12)$$

Eq. (12) establishes the relationship between the dynamic tension of the transmission conductor and the maximum jump height (between the uniced-coated conductor). It should be noted that Eq. (12) is an exact solution.

### E. SOLUTION BASED ON ENERGY PRINCIPLE

The potential energy of a conductor can be divided into two parts, one is the strain potential energy  $V_g$  generated by the horizontal tension, and the other one is the strain potential energy  $V_e$  generated by the dynamic tension. From state I to state II, it is obvious that the mass of covered ice has done work  $W$ . After the covered ice on the conductor completely falls off, i.e., from state II to state III, then the conductor finally stabilizes in state IV. According to the conservation of energy, the work done by gravity from state I to state II should be equal to the change of potential energy from state II to state III.

The static displacement distribution of the conductor after ice shedding is shown in Eq. (6), then the gravitational work done by the covered ice could be calculated as:

$$W = \frac{1}{2} \int_0^l m_1 g w dx = \frac{m_1 g l \Delta d}{3} \quad (13)$$

where  $\Delta d$  is the difference in sag at the midpoint before and after ice shedding. Obviously, the work done by the gravity from the covered-ice is transformed into the potential energy generated by state III and the strain potential energy generated by dynamic tension. The gravitational potential energy is given by:

$$V_g = \frac{1}{2} \int_0^l \left(\frac{\partial w}{\partial x}\right)^2 dx \quad (14)$$

where  $V_g = V_g / \{(mgl^2/H) mgl\}$ . For the small sag cable, the displacement distribution from state I to state III is given by Eq. (10), and it is also assumed that the maximum displacement at the midpoint of the span is  $A_0$ . Then it can be obtained by integrating  $V_g = \frac{1}{2} H \int_0^l \left(\frac{\partial w}{\partial x}\right)^2 dx$ , one can obtained:

$$V_g = \frac{H}{16l} (A_0)^2 \omega (\omega - \sin(\omega)) / \sin^4(\omega/4) \quad (15)$$

Similarly, the strain potential energy  $V_e = \frac{1}{2} \frac{mg}{H} \int_0^l h w dx$  generated by dynamic tension can be simplified as

$$V_e = \frac{H}{2l} (A_0)^2 \omega \left(\frac{\omega}{2} - \sin(\omega) + \frac{\omega}{2} \cos(\omega)\right) / \left(\cos\left(\frac{\omega}{2}\right) - 1\right)^2 \quad (16)$$



According to the conservation law of energy, ignoring the influence of damping force, it can be known that the increase in potential energy from state II to state III is equal to the work done by the equivalent load of ice during the process from state I to state II.

$$V_g + V_e = W \quad (17)$$

Substituting Eq. (17) into Eqs. (13), (14), and Eqs. (16) to (17), the amplitude expressions from state I to state III can be solved as:

$$A_0 = \left( \frac{m_1}{m} \Delta d d \right)^{0.5} \frac{\left( 1 - \tan\left(\frac{\omega}{2}\right) \sin\left(\frac{\omega}{2}\right) - \cos\left(\frac{\omega}{2}\right) \right)}{\omega \left( \frac{9\omega^2}{32\lambda^2} + \frac{3}{32} \tan^2\left(\frac{\omega}{2}\right) \right)^{0.5}} \quad (18)$$

It can be seen from Eq. (18) that the maximum jump height of the ice-covered transmission line is related to the initial sag  $d$  of the conductor, the ice-covered sag difference  $\Delta d$ , the dimensionless frequency  $\omega$ , and the ice-covered mass ratio  $m_1/m$ , and the last term of Eq. (18) is related to the dynamic characteristics of vibration. Finally, the total jump height from state II to state III is  $A_0 + \Delta d$ .

Assume that,

$$C = \frac{1 - \tan\left(\frac{\omega}{2}\right) \sin\left(\frac{\omega}{2}\right) - \cos\left(\frac{\omega}{2}\right)}{\left( \frac{9\omega^2}{32\lambda^2} + \frac{3}{32} \omega^2 \tan^2\left(\frac{\omega}{2}\right) \right)^{0.5}} \quad (19)$$

The Eq. (18) can be simplified as

$$A_0 = C \left( \frac{m_1}{m} \Delta d d \right)^{0.5} \quad (20)$$

#### IV. EXAMPLE VERIFICATION CALCULATION METHOD FOR JUMP HEIGHT

For TLs with a span of 550m, the cross-sectional area of the conductor is 621mm<sup>2</sup>, the density is 3090kg/m<sup>3</sup>, and the elastic modulus is 63GPa. The initial stress under the self-weight is 88.08Mpa, and the maximum sag at the midpoint of the span is 13m. When the ice thickness is 20mm, the density of icing is 3780kg/m<sup>3</sup>, and the stress after icing is 151.38Mpa.

In the current study, the finite-element LINK10 in ANSYS was used to simulate the conductor. LINK10 is a linear element with prestress, which can withstand axial tension. Each node has three degrees of freedom in X, Y and Z directions, and can be iteratively form-finding by applying initial strain. The insulator string is always in a tension state during the movement of the wire, and its stiffness is much higher than that of the wire, so the finite-element LINK8 is used for simulation of insulator. The self-weight of a conductor is evenly distributed along its length, and its initial configuration is catenary under the action of self-weight. The influence of the stiffness of the transmission tower on the deicing of the ice-covered TLs is ignored, and the fixed branch is used to simulate the freedom constraint of the insulator at the end of the tower.

In the analysis and modeling, covered-ice is directly simulated as the concentrated mass at the unit node, and finite-element Mass21 is used to simulate the concentrated mass.

In the simulation of deicing, the corresponding equivalent mass block at the unloading of the unit is simulated by controlling the life and death of the unit to simulate the simultaneous icing and chain shedding process.

According to the theoretical calculation proposed in the current study, the dimensionless parameter of the conductor  $\lambda^2$  is 25.6125, and the initial 1st-order dimensionless frequency is 5.45. The sag difference before and after icing is 3.83m, the jump height from state I to state III is 6.32m, and the total jump height is 10.147m. The work done by icing is 29343.7 N·m, the potential energy generated by the initial tension during the jumping process is 18775.9 N·m, and the potential energy generated by the dynamic tension from state II to state III is 10567.8 N·m, which satisfies the energy conservation. The ANSYS finite element numerical analysis result is 9.984m, which is 1.6% different from the deduction result in this paper. If considering the damping ratio of 0.4% for the conductor, the calculated jump height is 9.977m, which is 1.7% different from the result calculated by the method in the current study, and the difference is enlarged by 0.1%. It can be seen that the method proposed in this paper can accurately predict the maximum jump height after ice shedding, and the influence of the conductor-damping ratio can be ignored. Since the derivation in this paper is based on the basic energy principle, the calculation method can also be applied to the vibration of multi-level continuous conductors after ice shedding, only need to consider different frequency parameters.

#### A. PARAMETER ANALYSIS

According to Eq. (18), the influencing factors of maximum jump height for TLs after ice shedding are only related to the mass ratio, sag difference, vertical frequency, and dimensionless parameter  $\lambda^2$ . In the present study, those parameters are analyzed separately. For the convenience of comparison, the mass of the covered-ice and the mass of the conductor are taken to be the same, both are 1.919kg/m. It is assumed that the vertical-span ratio before icing remains unchanged, both of which are 42.31. Only the 1st-order modal frequency is discussed, and the dimensionless frequency and jump height of the TLs after ice shedding are shown in Fig. 2. It can be seen that with the same vertical span ratio, the larger the span, the lower the frequency. The maximum jump height also increases nonlinearly with the increase of the span length, showing a parabolic relationship. The theoretical solution of the formula derived in the current study is in good agreement with the numerical results of ANSYS.

As shown in Fig. 3, the jump height increases approximately linearly with the increase of the mass ratio of covered-ice. The theoretical results from the current method are in good agreement with the FEM results, indicating that the variable relationship between the jump height and the ice-covered mass ratio in Eq. (18) is precise. Of course, with the increase of the mass ratio, the dimensionless parameter  $\lambda^2$  of the conductor will increase synchronously, resulting in a slight nonlinearity in Eq. (18), and leading to an increase

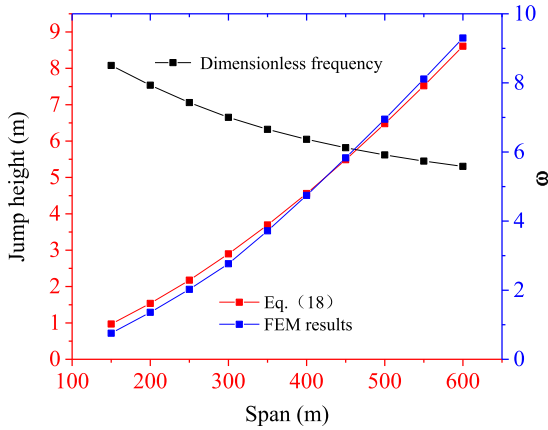


FIGURE 2. Relationship of jump height and span length.

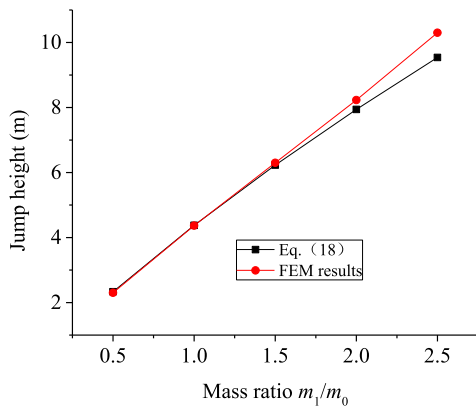


FIGURE 3. Relationship of jump height and mass ratio.

in error. In engineering applications, the ratio of icing mass to conductor mass rarely exceeds 2.5. Therefore, the relationship between jump height and mass ratio in the formula derived in the current study is also accurate.

The effect of the initial vertical-span ratio on the ice-covered jump is investigated with a span length of 400m. As shown in Fig. 4, with the increase of sag, the dimensionless frequency increases, while the maximum jump height decreases. The maximum jump height at the midpoint varies nonlinearly with the sag from the results of both the FEM and current method. The difference between Eq. (18) and ANSYS numerical simulation increases with the sag increase. According to the theory of cable structure [20], the high-order vertical frequency has a greater contribution to the dynamic tension for TLs with large vertical span ratios. Only considering the 1st-order frequency to calculate the response of TLs with a large vertical-span ratio after ice shedding may lead to larger calculation results.

Figure 5 shows the change of the dimensionless parameter  $C$  of the first two modes with different dimensionless parameters  $\lambda^2$ . With the vertical-span ratio increasing, the values of  $\lambda^2$  increases. The parameter  $C$  calculated in the 1st-order mode decreases nonlinearly with the dimensionless parameter  $\lambda^2$ , and tends to be stable when the  $\lambda^2$  is greater

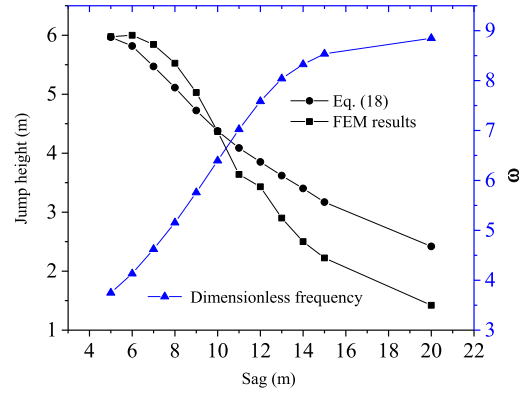


FIGURE 4. Relationship of jump height and cable sag.

than 400. Obviously, considering the 2nd-order mode will increase the dynamic tension of the conductor. When the  $\lambda^2$  is equal to about 150, the parameter  $C$  is close to 0. Similarly, when the  $\lambda^2$  is greater than 400, the value of  $C$  tends to be stable, and the effect of the 2nd-order mode on the jump height also tends to be stable.

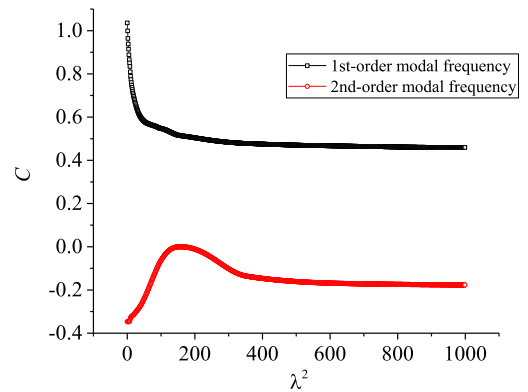


FIGURE 5. Parameter  $C$  calculated by the first two modal.

### B. MULTIMODAL CORRECTION

The main reason for the difference between the current theoretical formula and FEM simulation in the previous section is that only the influence of the 1st-order mode is considered. In addition, the derivation of the formula is based on linear theory, which is suitable for the case of small vertical-span ratios and large stress. Here, according to the theory of cable structure, the  $n$ -order modal dynamic tension participation coefficient  $\alpha_n$  is introduced, which is also the participation coefficient of the strain energy in the total energy [28].

$$\alpha_n = \frac{2/3}{[1 + \lambda^2 \{\tan(\omega_n/2) / (\omega_n/2)\}^2 / 12]} \quad (21)$$

In the engineering applications, the modal participation coefficients of the first eight orders can be obtained by Eq. (21). Then the proportion of the 1st order modal in the total strain energy can be obtained, and the amplitude correction coefficient can be calculated as the square root

relationship of the energy correction coefficient, as shown in Equation (22), so Equation (18) is modified.

$$\beta = \left( \frac{\alpha_1}{\sum_n \alpha_n} \right)^{0.5} \quad (22)$$

Fig. 6 presents the relationship between the amplitude correction coefficient and the dimensionless parameter  $\lambda^2$  when the first 8-order modes are considered. It can be found that with the increase of the parameter  $\lambda^2$ , the participation ratio of the higher-order modes increases and the correction coefficient decreases. The corrected maximum jump height is shown in Fig. 7. It can be seen that the results obtained by considering the participation of high-order modes can match well with the FEM results with a large sag.

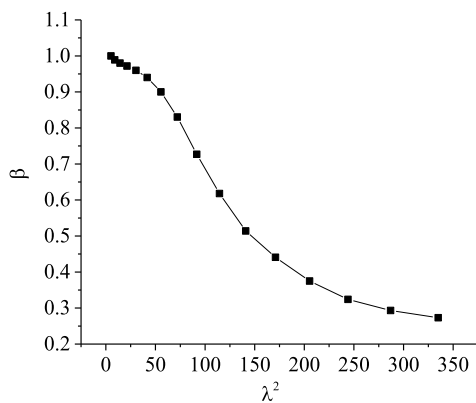


FIGURE 6. Amplitude correction factor.

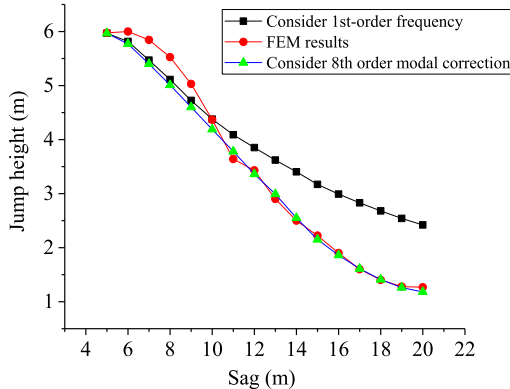


FIGURE 7. Modified results considering higher modes.

### C. DIMENSIONLESS PARAMETER FITTING

Since the modal correction method needs to consider the modal participation order, and it is inconvenient for engineering applications. Considering that  $C$  in Eq. (19) is related to the dimensionless parameter  $\lambda^2$  and the dimensionless frequency  $\omega$ , which are not independent with each other.

Therefore, with the undetermined coefficient method, only the dimensionless parameter  $\lambda^2$  is considered to log the

numerical values. The simulation results are fitted with parameters. Then the relationship between the dimensionless parameters  $C$  and  $\lambda^2$  can be obtained, which is a dimensionless relationship and has universal applicability. Finally, we get

$$C = 0.816e^{-0.076\lambda^2} \quad (23)$$

Combining Eq. (18), the maximum jump height can be expressed as follow:

$$A_0 = 0.816e^{-0.076\lambda^2} \left( \frac{m_1}{m} \Delta dd \right)^{0.5} \quad (24)$$

Obviously, Eq. (24) is a very simplified expression, which clearly expresses the laws of physical parameters in the process of icing and ice-shedding. The values of  $C$  with different  $\lambda^2$  calculated by Eq. (23) are also plotted in Fig. 8. It can be seen that the fitting result of the dimensionless parameters is relatively good when  $\lambda^2$  is less than 250. The above calculation example is also calculated, and the relationship between the maximum jump height and sag is obtained as shown in Figure 9. The results show that after adopting Eq. (24), the calculated results are also more accurate.

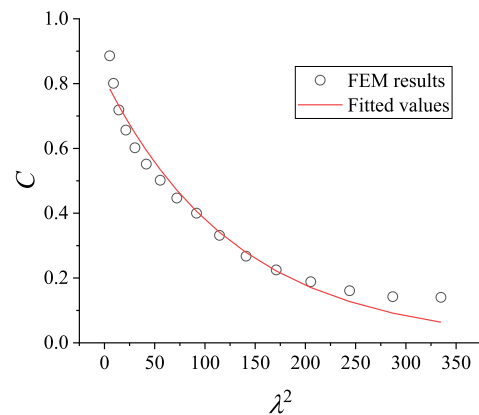


FIGURE 8. Variation of the dimensionless parameters  $C$  with  $\lambda^2$ .

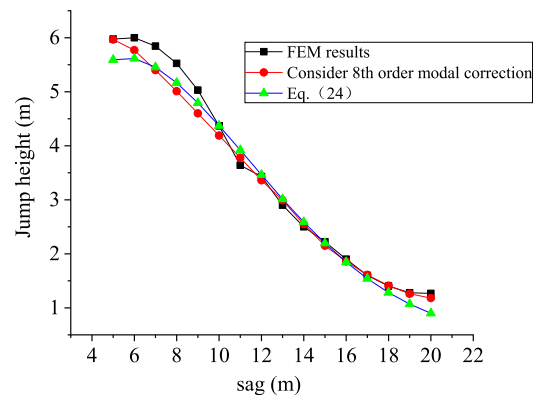


FIGURE 9. Comparison of jump heights with different methods.

According to Eq. (24), for multi-span and multi-bundle conductors, only the boundary conditions and structure of the cable lead to the change of the modal parameter  $\lambda^2$ .

The model proposed in the current study can be applied to vibration analysis after ice shedding for continuous multi-span and multi-bundle conductors.

## V. CONCLUSION

In this study, the maximum jump height of isolated-span ice-covered TLs is deduced based on cable structure theory and transmission line vibration energy method. The quantitative relationship among the maximum jump height of TLs after ice shedding and conductor sag, ice-covered sag difference, dimensionless frequency, and ice-covered mass ratio was investigated based on the energy principle. Then the analytical calculation formula for estimating the maximum jump height relative to the initial state of the conductor before icing is developed, by establishing a theoretical analysis simplified model of isolated span TLs after ice shedding. The following concluding remarks are drawn:

- 1) With the same vertical-span ratio, the larger the span of TLs, the lower the frequency. The maximum jump height of the conductor after ice shedding increases nonlinearly with the span length, approximately in a parabolic relationship. Since the sag after icing is also related to the icing mass, the ratio of maximum jump height to ice-covered mass is close to a linear relationship.
- 2) The maximum deicing jump height calculated by considering the 1st-order modal frequency is in good agreement with the FEM results with a small vertical span ratio. The total jump height calculated by the current method is only 1.6% lower than that from finite element method. If considering the damping ratio of 0.4% for the conductor, the jump height from FEM is about 1.7% larger than the result calculated by the current method, and the difference is enlarged by 0.1%.
- 3) The contribution of higher-order vertical modes to the dynamic tension needs to be considered with a larger vertical span ratio. The proposed correction coefficient can realize the correction of the maximum jump height after ice shedding considering the participation of higher-order modes.
- 4) A more simplified calculation formula of maximum jump height can be obtained with the exponential fitted dimensionless parameters, which can better reflect the physical law of maximum jump height of TLs after ice shedding.

## REFERENCES

- [1] Z. Yan, E. Savory, Z. Li, and W. E. Lin, "Galloping of iced quad-conductors bundles based on curved beam theory," *J. Sound Vib.*, vol. 333, no. 6, pp. 1657–1670, Mar. 2014.
- [2] Y. Zhong, S. Li, W. Jin, Z. Yan, X. Liu, and Y. Li, "Frequency domain analysis of alongwind response and study of wind loads for transmission tower subjected to downbursts," *Buildings*, vol. 12, no. 2, p. 148, Jan. 2022.
- [3] H. Aboshosha, A. Elawady, A. E. Ansary, and A. E. Damatty, "Review on dynamic and quasi-static buffeting response of transmission lines under synoptic and non-synoptic winds," *Eng. Struct.*, vol. 112, pp. 23–46, Apr. 2016.
- [4] E.-S. Abd-Elaal, J. E. Mills, and X. Ma, "A review of transmission line systems under downburst wind loads," *J. Wind Eng. Ind. Aerodyn.*, vol. 179, pp. 503–513, Aug. 2018.
- [5] F. Yang, J. Yang, J. Han, and D. Fu, "Dynamic responses of transmission tower-line system under ice shedding," *Int. J. Struct. Stability Dyn.*, vol. 10, no. 3, pp. 461–481, Sep. 2010.
- [6] V. T. Morgan and D. A. Swift, "Jump height of overhead-line conductors after the sudden release of ice loads," *Proc. Inst. Electr. Eng.*, vol. 111, no. 10, p. 1736, 1964.
- [7] M. R. Fekr and G. McClure, "Numerical modelling of the dynamic response of ice-shedding on electrical transmission lines," *Atmos. Res.*, vol. 46, nos. 1–2, pp. 1–11, Apr. 1998.
- [8] K. Wu, B. Yan, H. Yang, J. Lu, Z. Xue, M. Liang, and Y. Teng, "Dynamic response characteristics of isolated-span transmission lines after ice-shedding," *IEEE Trans. Power Del.*, vol. 38, no. 5, pp. 3519–3530, Oct. 2023.
- [9] G. Huang, B. Yan, N. Wen, C. Wu, and Q. Li, "Study on jump height of transmission lines after ice-shedding by reduced-scale modeling test," *Cold Regions Sci. Technol.*, vol. 165, Sep. 2019, Art. no. 102781.
- [10] M. Liu, Z. Yan, S. Feng, and Y. You, "Wind tunnel model tests for ice-shedding vibration of multi-span icing conductors," *J. Vib. Shock*, vol. 37, no. 3, pp. 223–229, 2018.
- [11] X. Meng, L. Wang, L. Hou, G. Fu, B. Sun, M. MacAlpine, W. Hu, and Y. Chen, "Dynamic characteristic of ice-shedding on UHV overhead transmission lines," *Cold Regions Sci. Technol.*, vol. 66, no. 1, pp. 44–52, Apr. 2011.
- [12] X. Long, X. Gu, C. Lu, Z. Li, Y. Ma, and Z. Jian, "Prediction of the jump height of transmission lines after ice-shedding based on XGBoost and Bayesian optimization," *Cold Regions Sci. Technol.*, vol. 213, Sep. 2023, Art. no. 103928.
- [13] A. Jamaledine, G. McClure, J. Rousselet, and R. Beauchemin, "Simulation of ice-shedding on electrical transmission lines using adina," *Comput. Struct.*, vol. 47, nos. 4–5, pp. 523–536, Jun. 1993.
- [14] L. E. Kollar and M. Farzaneh, "Vibration of bundled conductors following ice shedding," *IEEE Trans. Power Del.*, vol. 23, no. 2, pp. 1097–1104, Apr. 2008.
- [15] B. Yan, K. Chen, Y. Guo, M. Liang, and Q. Yuan, "Numerical simulation study on jump height of iced transmission lines after ice shedding," *IEEE Trans. Power Del.*, vol. 28, no. 1, pp. 216–225, Jan. 2013.
- [16] K. Ji, X. Rui, L. Li, A. Leblond, and G. McClure, "A novel ice-shedding model for overhead power line conductors with the consideration of adhesive/cohesive forces," *Comput. Struct.*, vol. 157, pp. 153–164, Sep. 2015.
- [17] K. Ji, X. Rui, L. Li, C. Zhou, C. Liu, and G. McClure, "The time-varying characteristics of overhead electric transmission lines considering the induced-ice-shedding effect," *Shock Vib.*, vol. 2015, pp. 1–8, Jan. 2015.
- [18] C. Wu, B. Yan, L. Zhang, B. Zhang, and Q. Li, "A method to calculate jump height of iced transmission lines after ice-shedding," *Cold Regions Sci. Technol.*, vol. 125, pp. 40–47, May 2016.
- [19] S. Gao, C. Zeng, L. Zhou, X. Liu, and B. Gao, "Numerical analysis of the dynamic effects of wine-cup shape power transmission tower-line system under ice-shedding," *Structures*, vol. 24, pp. 1–12, Apr. 2020.
- [20] L. Zhongbin, X. Liu, B. Zhang, T. Yaguang, F. Li, L. Qing, and B. Yan, "Dynamic characteristic of conductor after ice-shedding and simulation analysis of the tension insulator string," *IEEE Access*, vol. 10, pp. 118484–118497, 2022.
- [21] L. E. Kollar and M. Farzaneh, "Modeling sudden ice shedding from conductor bundles," *IEEE Trans. Power Del.*, vol. 28, no. 2, pp. 604–611, Apr. 2013.
- [22] N. Wen, B. Yan, Z. Mou, G. Huang, H. Yang, and X. Lv, "Prediction models for dynamic response parameters of transmission lines after ice-shedding based on machine learning method," *Electr. Power Syst. Res.*, vol. 202, Jan. 2022, Art. no. 107580.
- [23] H. Oertli, "Oscillations de cables electriques aeriens apres la chute de surcharges," *Bull. Assoc. Suisse Electr.*, vol. 41, no. 5, pp. 501–511, 1950.
- [24] V. List and K. Pochop, "Mechanical design of overhead transmission lines," SNTL Publisher Tech. Literature, Prague, Czech Republic, 1963.
- [25] *Design Manual of High Voltage Transmission Lines for Electric Engineering*, China Electr. Power Press, Beijing, China, 2003.
- [26] X. Xie, Y. Wu, K. Liang, S. Liu, and J. Peng, "Experiment study on dynamic effects of tower-line systems induced by ice shedding," *Adv. Civil Eng.*, vol. 2020, pp. 1–9, Feb. 2020.



- [27] W.-J. Lou, Y.-L. Zhang, H.-W. Xu, and M.-F. Huang, "Jump height of an iced transmission conductor considering joint action of ice-shedding and wind," *Cold Regions Sci. Technol.*, vol. 199, Jul. 2022, Art. no. 103576.
- [28] H. M. Irvine, *Cable Structures*. Cambridge, MA, USA: MIT Press, 1981.
- [29] J. Si, L. Zhou, K. Zhu, H. Zhao, B. Liu, X. Rui, and S. Liu, "Dynamic response of tension plate for UHVDC transmission lines under ice shedding loads," *CSEE J. Power Energy Syst.*, vol. 8, no. 3, pp. 952–962, May 2022.
- [30] Z. Ye, C. Wu, X. Liu, and F. Huang, "Numerical simulation of the dynamic responses of electric power fitting of transmission lines after ice shedding," *Shock Vib.*, vol. 2022, pp. 1–28, Jun. 2022.

**JINYU WANG** received the M.Sc. degree. Her main research interests include power distribution systems, fault processing, and physical simulation.



**YONGLI ZHONG** was born in China. He received the B.S. degree from the Huazhong University of Science and Technology and the Ph.D. degree in civil engineering from Chongqing University. His research interests include the response of the transmission line under the downburst and ice shedding of the conductor.



**MING LU** was born in China. He received the M.S. degree. His research interests include the galloping of transmission lines and high voltage external insulation of overhead lines.



**ZHITAO YAN** was born in China. He received the M.S. and Ph.D. degrees from Chongqing University. He is currently a Professor. His research interests include the galloping of transmission lines and dynamics of structures.



**BIN LIU** received the D.Sc. degree in mechanical engineering from the Chinese Academy of Science, Beijing, China, in 2007. His current research interest includes the theory and technology of the mechanical security of overhead transmission lines impacted by wind, rain, and ice loads. He is currently a member of the Technical Advisory Group of CIGRE B2-AG-06 and a member of the Task Group of CIGRE WGB2.46.

...